Case Studies in Chemical and Environmental Engineering 11 (2025) 101094

Contents lists available at ScienceDirect

Case Studies in Chemical and Environmental Engineering

journal homepage: www.sciencedirect.com/journal/case-studies-in-chemical-and-environmental-engineering

Case Report

The thermal-flow performance of water-Al_2O_3 nanofluid flow in an elliptical duct heat exchanger equipped with two rotating twisted tapes

Hassan Wathiq Ayoob [a], Ihab Omar [b], Wed khalid Ghanim [a], Mohammad N. Fares [a], Mohammad Ali Fazilati [c,**], Soheil Salahshour [d,e,f], Sh Esmaeili [g,*]

[a] Chemical Engineering Department, University of Basrah, Basrah, 61001, Iraq
[b] Air Conditioning Engineering Department, Faculty of Engineering, Warith Al-Anbiyaa University, Karbala, 56001, Iraq
[c] Department of Mechanical Engineering, Khomeinishahr Branch, Islamic Azad University, Khomeinishahr, Iran
[d] Faculty of Engineering and Natural Sciences, Istanbul Okan University, Istanbul, Turkey
[e] Faculty of Engineering and Natural Sciences, Bahcesehir University, Istanbul, Turkey
[f] Faculty of Science and Letters, Piri Reis University, Tuzla, Istanbul, Turkey
[g] Faculty of Physics, Semnan University, P.O. Box: 35195-363, Semnan, Iran

ARTICLE INFO

Keywords:
Nanofluid flow
Elliptical duct heat exchanger
Rotating twisted tapes
Numerical analysis
Nusselt number

ABSTRACT

Background: The thermal-flow performance of nanofluid (*NF*) flow in an elliptical duct heat exchanger fitted and turbulated with two rotating tapes is investigated. The issues concerning rotating twisted tapes inside the oval tubes using *NF* as the working fluid simulated with two-phase modeling have received less attention in previous studies.
Methods: Considering the importance of employing the heat transfer improving methods in tubular heat exchangers, the passive and ative heat transfer improving methods examined here. As a novel study case, the rotated tapes beside the water-Al_2O_3 *NF* of was used; and sensitivity analysis was performed to reveal the effect of the volume fraction of nanoparticles (ϕ), tapes rotational speed and Re number on the *Nu* number, pumping power and figure of merit (*FOM*). The heat flux of 5000 Wm^{-2} was applied to the wall surface, and the two-phase mixture method was employed for the simulation. The heat exchanger performance is studied in cases of fixed and rotating twisted tapes with three different rotational speeds. The results show that increasing the Re number, ϕ and the rotation speed of the blades would increase the *Nu* number and pumping power in all cases. The increase in ϕ improves the *Nu* number by 6.1 %–19.4 % and the pumping power by 59.2–280 %. The *Nu* number change by increasing ϕ is lower at low Re numbers and becomes higher at high Re numbers. The effect of ϕ increment on heat transfer is increasing but took place with a higher inclination rate in rotating tapes rather than stationary tapes and plain tube cases. In the cases of rotated twisted tape mode, the value of *FOM* is always greater than one and is below 0.9 for stationary mode.
Significant findings: The highest value of *FOM* is 1.57, which is for the highest rotational speeds, the lowest Re number, and $\phi = 1$ %. Increasing the Re number reduces the *FOM* while increasing ϕ improves it.
Practical significance and potential area of application: The increasing need for efficient heat transfer in heat exchanger devices necessitated the application of heat transfer augmentation techniques. The effects of twisted tapes, their rotation, and the application of *NFs* in heat exchangers as the active and passive heat transfer increment methods are studied numerically.

* Corresponding author.
** Corresponding Author
E-mail addresses: fazilati@iaukhsh.ac.ir (M.A. Fazilati), shadi.esmaili@iaukhsh.ac.ir (S. Esmaeili).

https://doi.org/10.1016/j.cscee.2025.101094
Received 23 December 2024; Received in revised form 31 December 2024; Accepted 1 January 2025
Available online 3 January 2025

Nomenclature

Abbreviations	
a	cent to cent length of channel (m)
c_p	specific heat capacity (kJ/kg.°C))
D	diameter
E	total energy (kJ)
FOM	figure of merit
FVM	finite volume method
h	specific enthalpy (kJ/kg), height (m)
h_{TT}	height of the twisted tape
h_x	convective local heat transfer coefficient
HTF	heat transfer fluid
k	thermal conductivity (W/m.K)
L	length (m)
LHS	latent heat storage
NF	nanofluid
NP	nanoparticle
Nu	Nusselt number
p	pressure (kPa)
PCM	phase change material
PT	plain tube
QUICK	Quadratic upstream interpolation for convective kinetics differencing scheme
$\ddot{q}$	Heat flux (W/m^2)
r	radius of channel (m)
RTT1	rotating twisted tape 1 mode
RTT2	rotating twisted tape 2 mode
RTT3	rotating twisted tape 3 mode
Re	Reynolds number
SIMPLE	
STT	stationary twisted tape
SHS	sensible heat storage
T	temperature (K)
TiO_2	titanium oxide
TT	twisted tape
TES	thermal energy storage
u	axial velocity (m/s)
$\dot{V}$	volume flow rate (m^3/s)
V	velocity (m/s)
$\dot{W}$	pumping power (μW)
Z^*	dimensionless length of duct
Greek symbols	
Δ	difference
ε	tape thickness
φ	the volume fraction of nanoparticles
μ	dynamin viscosity (Pa.s)
ω	rotational speed (rad/s)
ρ	density (kg/m^3)
Subscripts	
avg	average value
b	bulk
eff	effective
f	fluid, base fluid
h	hydraulic
i	inlet flow
loc	local value
m	mixture
nf	nanofluid
p	particle
t	turbulent
w	wall

1. Introduction

Industrial development relies heavily on the application of heat exchangers [1,2]; the wide range of application of heat exchangers in industries such as food [3,4], oil, gas, and petrochemical industries made their heat transfer improvement an inevitable task. Although heat transfer improvements can be made in active or passive ways, by their large benefits, passive mechanisms have drawn substantial attention. Using turbulators [5,6] twisted tapes [7,8], drainage inserts [9], and vortex generators [10] are the most popular passive ways to enhance heat transfer. Due to its low cost, ease of manufacture, and simple installation, twisted tape (*TT*) inserts are the most common passive technique for enhancing heat transfer in heat exchangers [11]. By their special forms, the twisted tapes and their possible rotation would induce some level of turbulence which has heat transfer improving effect. Dewan [12] reviewed twisted tape and wire coil insert applications and concluded that twisted tape and wire coils are more efficient under laminar and turbulent flow regimes, respectively. Many studies have proposed mechanisms to enhance the heat transfer characteristics of twisted tapes [7,8]; using V-cut and square-cut twisted tapes [13,14] alternating clockwise and counter-clockwise twisted tapes [15] using wing part at the edge of the twisted tape [16] perforated [17] and center-cleared twisted tapes [18] and the rotating twisted tapes [19] are among these mechanisms. In all the above mentioned studies, the main goal was to achieve the highest heat transfer improvement and the lowest pressure drop increment.

Another heat transfer-improving passive method in heat exchangers is the use of metal or nonmetal nanoparticle (*NP*) suspensions, called nanofluid (*NF*), as the working fluid. Rashidi et al. [20] studied a square channel fitted with complex lateral buffers and found that increasing the volume fraction of nanoparticles (ϕ) increases the heat transfer rate. Jafaryar et al. [21] studied the effect of using *NF* on enhancing the heat transfer rate in a tube with twisted tapes. Their results revealed that the twisted tapes with higher twist angles increase the Nusselt number. Esfe et al. [22] analyzed *NF* flow in a pipe fitted with twisted tapes. They found that increasing the Re number reduces the friction factor. Qi et al. [23] investigated the effect of twisted tapes in a pipe with water/TiO_2 *NF* flow. Their results show that using rotating twisting increases the rate of heat transfer significantly. He et al. [24] evaluated the flow in a tube fitted with twisted tapes. Bahiraei et al. [25] investigated the *NF* flow and heat transfer in a pipe fitted with twisted tapes and concluded that increasing ϕ increases the heat transfer and $\dot{W}_{pump}$. El Magid Mohamed et al. [26] conduted an experimental and three dimensional numerical simulation transitional on double-tube heat exchanger with rotating inner tube; they examined different flow rate and *NF* types. They reported a heat exchanger efficiency increment for *NF* concentration up to 3 % with the highest improvement of 19.33 %. Heat transfer enhancement was 41.2 % for the tube rotation of 500 rpm. Ghazanfari et al. [27] investigated numerically the NF effect on twisted tubes efficiency at various pitch lengths using the *CFD*. The sensitivity analysis was made to reveal the effect of flow rete on *Nu* number, temperatures, and pressure drop. They found the outstanding effect of nanofluids application on heat transfer performance of system. Also, the twisted tube enhanced the heat transfer rate up to 1.12 times over smooth tube.

The literature survey shows that issues concerning rotating twisted tapes inside the oval tubes while using *NF* as the working fluid have received less attention. In addition, the two-phase modeling of *NF* flow in rotational flows has also been somewhat neglected in previous studies. This work studies the effect of rotating twisted tapes on the thermal performance of a heat exchanger in which *NF* is employed as the working fluid. The system performance was investigated in different working conditions: the channel with no internal tape (plain tube, *PT case*), the stationary twisted tape (*STT case*), and the rotating twisted tape (*RTT case*); the *RTT* case investigated in three different rotational speeds, denoted by *RTT1*, *RTT2*, and *RTT3* cases. In the next section, after explaining the problem and governing equations, the numerical procedures are described. The thermal and flow characteristics are visualized by the relevant contours and finally in the last section, the conclusions are drawn.

2. Setup and theoretical consideration

The schematic of the problem is shown in Fig. 1. The duct section is oval-shaped and fitted with two twisted tapes; the pitch of the tapes is equal to the tube length, and their height (h_t in Fig. 1) is 90 % of the channel height. The twisted tapes rotate with the rotational speed specified by the flow Re number. The workig fluid is NF of water/Al_2O_3. The dimensions of the channel and the tapes are shown in Table 1;

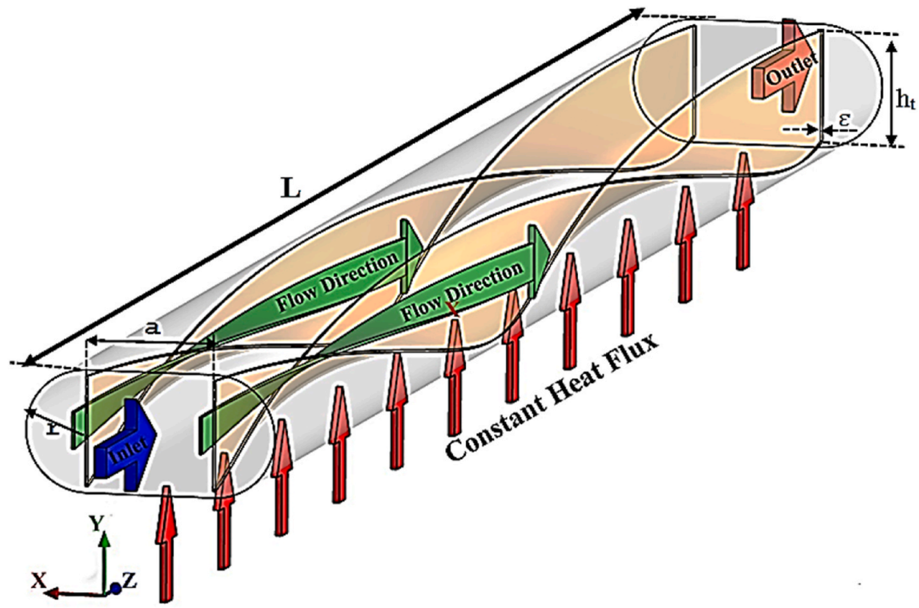

Fig. 1. The schematic of the problem.

Table 1
The dimensions of the tapes and channel.

Parameter	Value (mm)	
L	400	
a	21	
r	10	
ε	0.4	
h_t	18	
	Water	Al_2O_3
ρ (kg/m^3)	998.2	3880
c_p (J/kg.K)	4182	733
k (W/m.K)	0.6	36
μ (Pa.s)	0.0010	–

Table 2
Thermo-physical properties of the *NF* for different ϕ

Property	Equation	Value		
		$\phi = 1\%$	$\phi = 2\%$	$\phi = 3\%$
Density [30]	$\rho_{nf} = (1-\phi)\rho_f + \phi\rho_p$	1084.6540	1055.8360	1027.018
Specific heat [30]	$\rho_{nf} = C_{p,bf}\left((1-\phi)(\rho C_p)_f + \phi(\rho C_p)_p\right)$	4078.53	4113.02	4147.51
Thermal conductivity [30]	$k_{nf} = k_f(1 + 2.72\,\phi + 4.97\,\phi^2)$	0.6516	0.6338	0.6166
Dynamic viscosity [30]	$\mu_{nf} = \frac{\mu_f}{(1-\phi)^{2.5}}$	0.0013	0.0012	0.0011

moreover, the properties of pure water and Al_2O_3 particles are shown [29].

The thermophysical properties of *NF* are functions of those of the base fluid and ϕ. In all study cases, the fluid flow is considered Newtonian and is modeled using the finite volume method (*FVM*) [28]. The simulations were performed for Re numbers of 250, 500, 750, and 1000. The outer wall of the channel is subjected to $q'' = 5000$ Wm^{-2}. It should be noted that considering the goal of this study which is to show the improving effect of different passive techniques in an elliptical channel, the type of *NP* does not matter. The rotational speed of twisted tapes is

Table 3
The inlet velocities for the study cases.

ϕ (%)	Re	V_{inlet} (m/s)
1	250	0.009458
1	500	0.018917
1	750	0.028375
1	1000	0.037834
2	250	0.010132
2	500	0.020264
2	750	0.030396
2	1000	0.040528
3	250	0.010973
3	500	0.021945
3	750	0.032918
3	1000	0.043890

obtained as follows [29];

$$Re = \frac{\rho_{nf} V_{inlet} D_h}{\mu_{nf}} \tag{1}$$

$$\omega = \frac{2\,V_{inlet}}{h_{TT}} \tag{2}$$

where the hydraulic diameter D_h is determined using Eq. (3) [29],

$$D_h = \frac{4(\pi r^2 + 2ra)}{(2\pi r + 2a)} \tag{3}$$

The rotational speed of twisted tapes in the *RTT1 case* is obtained by Eq. (2) and the corresponding values in the *RTT2* and *RTT3 cases* are twice and triple the *RTT1* speed, respectively. The continuity, momentum, and energy equations can be written as follows [40]:

$$\vec{\nabla}.\left(\rho_m \vec{V}_m\right) = O \tag{4}$$

$$\vec{\nabla}.\left(\rho_m \vec{V}_m \vec{V}_m\right) = -\vec{\nabla}P + \vec{\nabla}.\left[\mu_m\left(\vec{\nabla}\vec{V}_m + \vec{\nabla}\vec{V}_m\right)\right] + \rho_m\vec{g} + \vec{F} - \vec{V}.\left(\sum_{k=1}^{n} \varnothing_k \rho_k \vec{V}_{dr.k} \vec{V}_{dr.k}\right) \tag{5}$$

where,

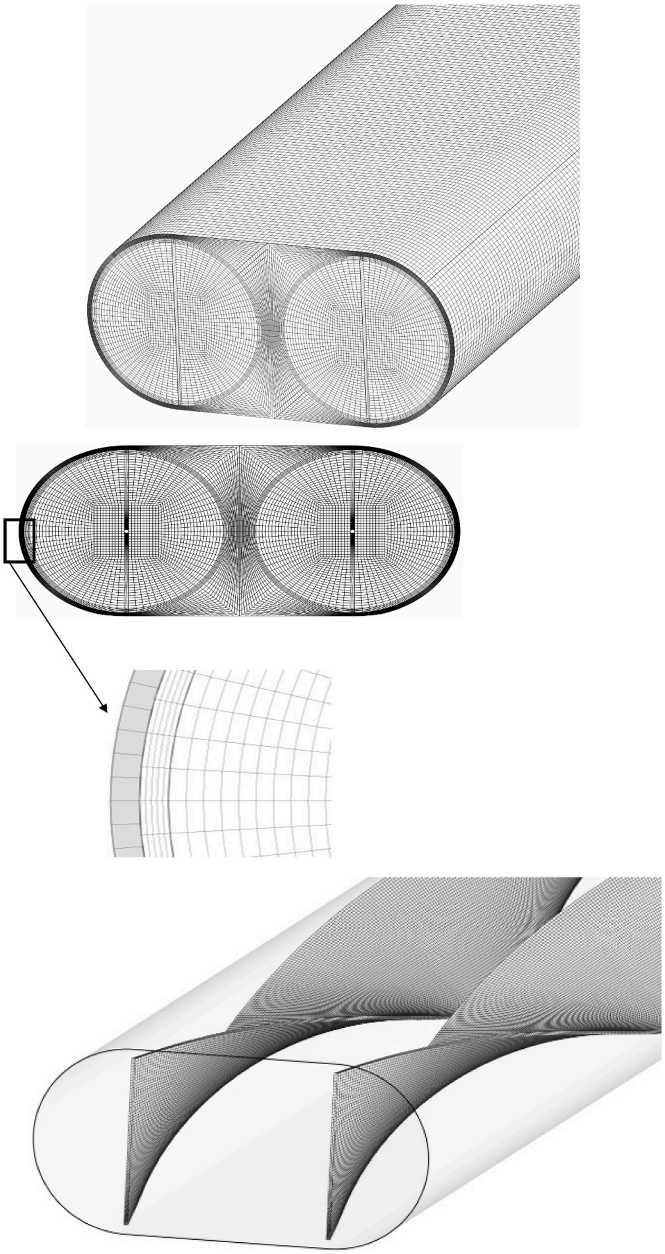

Fig. 2. The computational mesh.

$$\vec{V}_{dr.k} = \vec{V}_k - \vec{V}_m \tag{6}$$

$$\vec{\nabla}\cdot\left[\sum_{k=1}^{n}\left(\rho_k C_{p,k}\right)\overrightarrow{\phi_k}\,\vec{V}_k T\right] = \vec{\nabla}.k_m\vec{\nabla}T \tag{7}$$

$$\vec{V}_m = \frac{\sum_{k=1}^{n}\phi_k\rho_k\vec{V}_k}{\rho_m} \tag{8}$$

Additionally [29],

$$\rho_m = \sum_{k=1}^{n}\phi_k\rho_k \tag{9}$$

$$\vec{V}_{\rho f} = \vec{V}_\rho - \vec{V}_f \tag{10}$$

and,

$$\vec{V}_{dr.p} = \vec{V}_{pf} - \sum_{k=1}^{n}\frac{\phi_k\rho_k}{\rho_m}\vec{V}_{fk} \tag{11}$$

$$\mu_m = \sum_{k=1}^{n}\phi_k\mu_k \tag{12}$$

and,

$$\vec{V}_{pf} = \frac{\rho_p d_p^2(\rho_p - \rho_m)}{18\mu_f f_{drag}\rho_p}\left(\vec{g} - \left(\vec{V}_m.\vec{\nabla}\right)\vec{V}_m\right) \tag{13}$$

$$f_{drag} = \begin{cases} 1 + 0.15Re_p^{0.687} & (Re_p \le 1000) \\ 0.0183Re_p & (Re_p \le 1000) \end{cases} \tag{14}$$

Therefore,

$$\vec{V}_{dr.P} = \vec{V}_{pf} - \sum_{k=1}^{n}\left(\frac{\phi_k\rho_k}{\rho_m}\vec{V}_{fk}\right) \tag{15}$$

To determine the *NF* properties, some correlations are incorporated by which the thermo-physical properties are calculated, as listed in Table 2.

The pumping power ($\dot{W}_{pump}$) and Nu_{avg} are determined as follows [29]:

$$\dot{W}_{pump} = \dot{V}\Delta P \tag{16}$$

$$Nu_{loc} = \frac{h_x D_h}{k_{nf}} \tag{17}$$

and,

$$h_{loc} = \frac{q''}{T_w - T_b} \tag{18}$$

$$T_b = \frac{\sum(\dot{m}T)}{\sum\dot{m}} \tag{19}$$

$$Nu_{avg} = \frac{1}{L}\int_0^L Nu_{loc}dx \tag{20}$$

The figure of merit criterion (*FOM*) is used to evaluate the thermal efficacy [30]. Additionally, the non-dimensional length of the tube is defined by Eq. (22),

$$FOM = \frac{\frac{Nu}{Nu_{PT}}}{\left(\frac{\dot{W}}{\dot{W}_{PT}}\right)^{\frac{1}{3}}} \tag{21}$$

$$Z^* = \frac{Z}{L} \tag{22}$$

3. Numerical analysis

The governing equations using the mentioned boundary conditions are solved using the *FVM*. To discretize the governing equations, the *QUICK* and central differencing schemes are used. For coupling the pressure and velocity fields, the *SIMPLE* algorithm was used which had been proved to model the flow and heat transfer correctly [31]. The convergence criteria for the conservation equations was given 10^{-8} for all governing equations [19]. The boundary conditions over the system boundaries are as follows; the 300 *K* constant temperature condition was set for the inlet; also, the inlet velocities are listed in Table 3.

At the outlet, the outlet pressure condition equal to atmospheric pressure was set, and the velocity and temperature gradient were both set to zero there. For the walls, the no-slip condition is applied with an

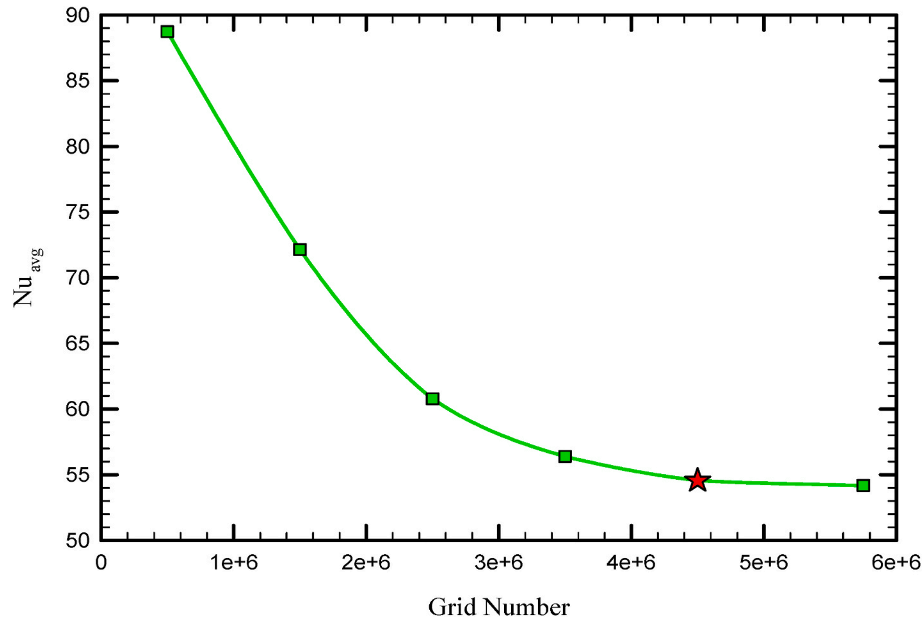

Fig. 3. Grid independency study in the *RTT3 case* and $\phi = 3$ % and Re = 1000 [45].

Table 4
Nu_{avg} for different numbers of elements in $\phi = 3$ % and Re = 1000.

Number of elements	Nu_{avg}	Error (%)
500000	89.250	–
1500000	71.889	19.5
2500000	61.721	14.1
3500000	56.400	8.6
4500000	54.957	2.6
5500000	54.175	1.4

exerted heat flux of 5000 Wm^{-2}. Additionally, thermal insulation and no-slip conditions are considered for the tape surface [19]. The assumption of no-slip condition is conventionally applied on the solid surface in viscous fluid flows; also, the thermal insulation condition "thin plate assumption" for the tapes surface and no heat out-flow from them. The following assumptions were used through the simulation [19].

- Steady, incompressible, and Newtonian flow;
- Two-phase fluid flow;
- Impacts of nanoparticle aggregation or stability on thermal performance were neglected.

Fig. 2 presents the structured mesh used in this study. As shown the tapes are in fact metal belt which twisted along the tube length and forms a wavy structure. The meshing was performed using Gambit and, the commercial software package of *ANSYS* Fluent has been employed

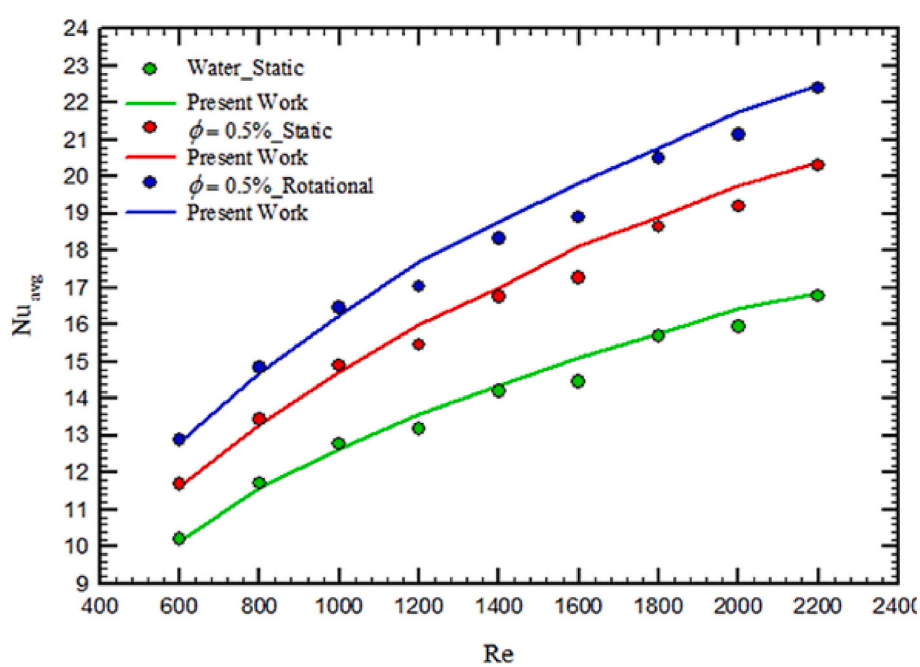

Fig. 4. Verification of present work by Ref. [23].

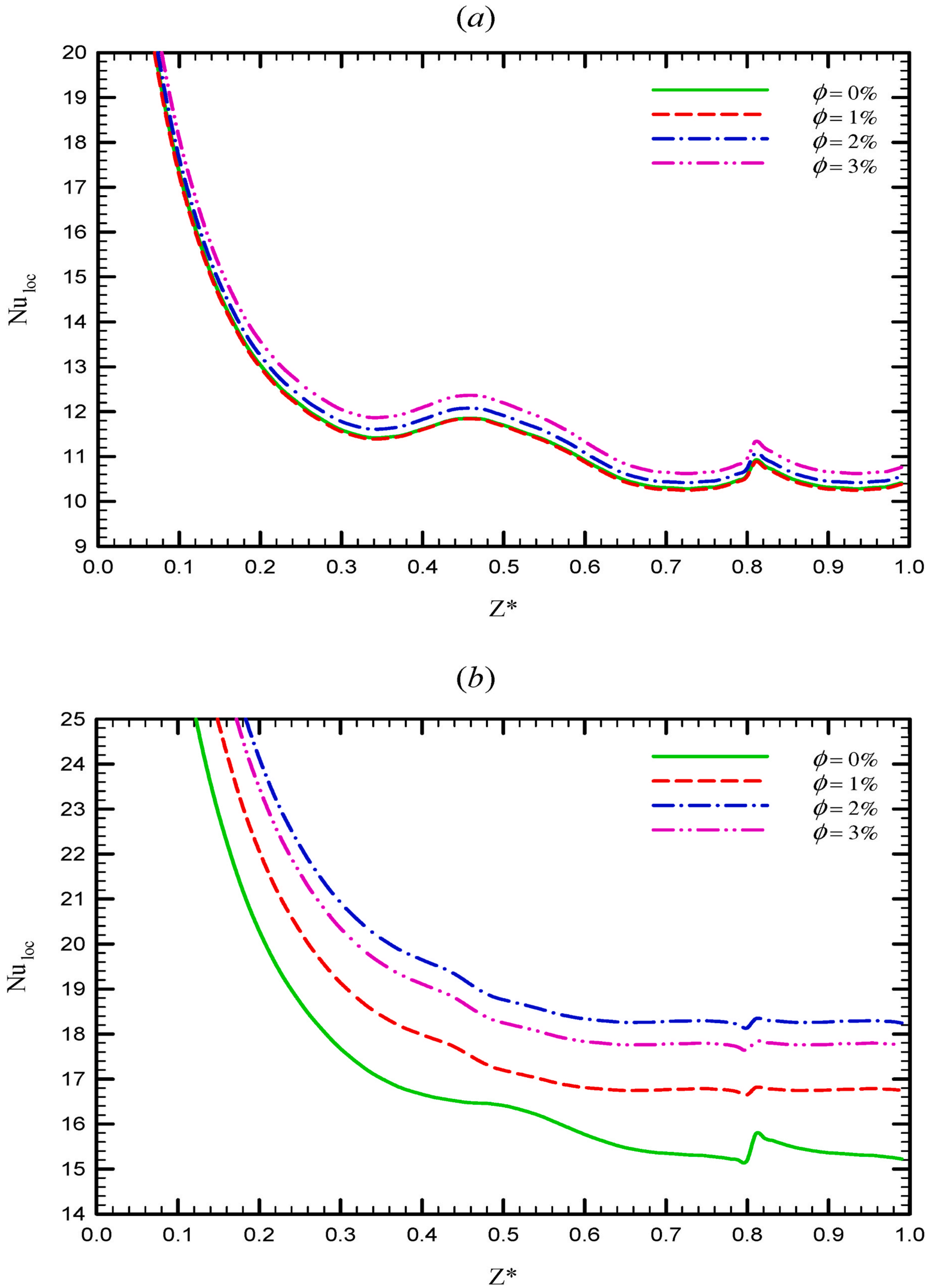

Fig. 5. $\boldsymbol{Nu_{loc}}$ in case of *STT case* and *a*) Re = 250 and *b*) Re = 1000, for different $\boldsymbol{\phi}$

(*a*)

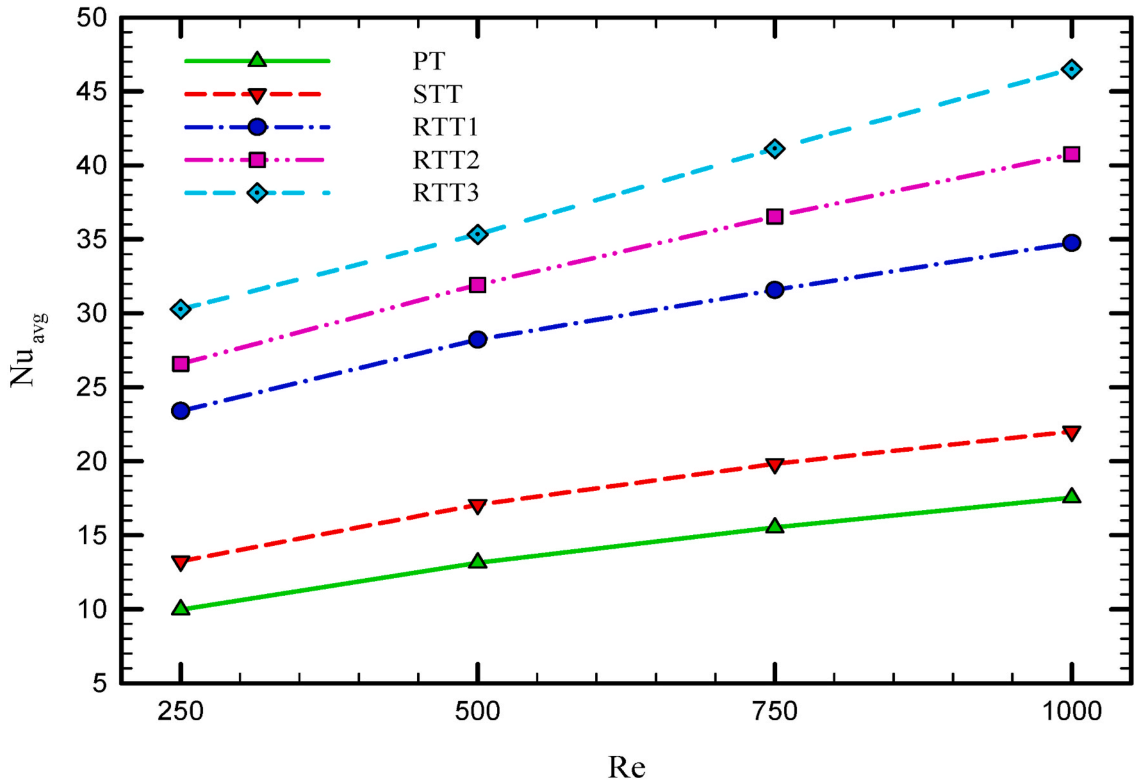

(*b*)

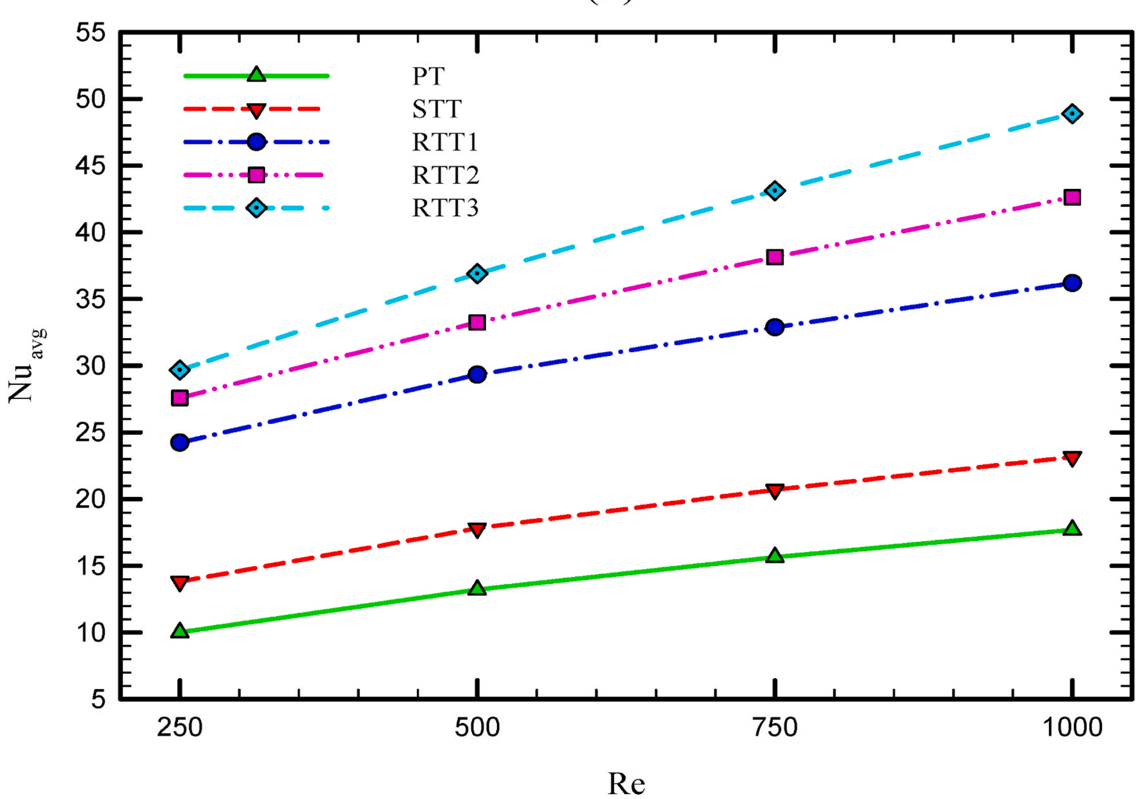

Fig. 6. $\boldsymbol{Nu_{avg}}$ versus the Re number in different cases and *a*) $\phi = 1$ % and *b*) $\phi = 3$ %.

Table 5
Nu_{avg} for different cases and Re numbers in $\phi = 1$ % and $\phi = 3$ %.

Re	PT	STT	RTT1	RTT2	RTT3
	Mode				
	ϕ = 1 %				
250	10.249	13.288	23.391	26.581	29.300
500	13.498	17.053	28.212	31.911	35.327
750	15.959	19.812	31.574	36.544	41.120
1000	18.030	22.325	34.750	40.750	46.492
$\frac{\Delta Nu_{ave}}{Nu_{ave}}\%$	76	68	49	53	59
Re	Mode				
	ϕ = 3 %				
250	10.030	13.802	24.450	28.060	30.066
500	13.102	18.112	29.503	32.501	37.502
750	16.021	20.982	33.270	48.029	43.201
1000	18.210	23.301	36.603	43.123	49.010
$\frac{\Delta Nu_{avg}}{Nu_{avg}}\%$	82	69	50	54	63

for simulation.

To approve the independency of the obtained result from the computational mesh, Nu_{avg} was evaluated in different mesh sizes and was compared with each other; the chosen mesh sizes were 500, 1500, 2500, 3500, 4500 and 5500 for whom Nu_{ave} determined; the selected mesh is that for which the difference between the obtained Nu_{ave} and the previous one is below 3 %. Fig. 3 shows Nu_{avg} versus the grid number for the *RTT3* case and $\phi = 3\%$ and Re = 1000; the corresponding numerical values are listed in Table 4. It seems that after four stages of cell miniaturization, no significant changes were observed in the value of the Nu_{avg}, and the changes to the next step are less than 3 %. Therefore, the domain with 4,545,000 elements was chosen for the ongoing simulations.

4. Results and discussion

As one of the evaluation indexes in studying the heat transfer performance, the local and average *Nu* numbers, denoted by Nu_{loc} and Nu_{ave}, respectively are investigated. To study the fluid flow characteristics, $\dot{W}_{pump}$ is used and presented. The studies are performed in working conditions of *PT*, *STT*, *RTT1*, *RTT2*, and *RTT3* cases using different ϕ. Last, to unveil the overall possible improvement effect of using the tapes, the *FOM* parameter is presented, and its value is compared between the study cases. To verify the numerical method, the simulation results were compared to the results of Qi et al. [23]. The base fluid was water in a tube fitted with twisted tape and Re numbers of 600 through 2200. Fig. 4 compares the Nu_{avg} obtained in this study and the previous experimental work; it could be seen that the present numerical simulation has good overlap with the experimental work with a maximum deviation of 4.9 %; since a difference of 15 % is acceptable in comparison with experimental works, the present simulation method would be approved [22].

4.1. The heat transfer performance

- *The variation of local Nu number*

Fig. 5 shows the value of Nu_{loc} for *STT case* and different ϕ values at Re =250 and 1000, respectively. For all Re numbers, growing ϕ increases Nu_{loc}, which is mainly due to the enhanced thermal properties of *NF*. The increased heat transfer coefficient due to the ϕ increase is due to the enhanced diffusion mechanism in *NF,* which reduces the heat penetration resistance from the walls to the bulk fluid [29]. Furthermore, the *Nu* number increased as a result of increasing ϕ is lower at low Re numbers; by increasing ϕ from $\phi = 0$ to $\phi = 4$ % at $Z^* = 0.5$, Nu_{loc} increases by 6 % and 13.5 % for Re = 250 and 1000, respectively. This verifies the effect of the inlet flow rate on improving the effect ϕ increment.

- *The variation of average Nu number; the effect of Re number*

Fig. 6 (a) shows the variation of Nu_{avg} versus the Re number in different working modes in $\phi = 1$ %. The minimum Nu_{avg} of 10.25 corresponds to Re number of 250 in the *PT* case and the maximum Nu_{avg} = 46.49 corresponds to Re = 1000 in the *RTT3* case. The Nu_{avg} in the *PT* case and Re = 250, 500, 750, and 1000 are 10.25, 13.50, 15.96, and 18.03, respectively; the corresponding values for the other cases are listed in Table 5. The percent change in the *Nu* number (ΔNu_{avg} %) between the minimum and maximum *Re* numbers for different cases is also shown in Table 5. As shown, the effect of increasing the Re number on altering the *Nu* number is not the same in different cases; in the *PT* case, increasing the Re number from its minimum to maximum value has the largest effect on the value of Nu_{avg} (76 % increment), while it is the smallest in the *RTT* case (49 % increment in the *RTT1 case*); additionally, for $\phi = 1$ %, the average improvement is 76 %.

In Fig. 6 (b) the value of Nu_{avg} versus the Re number in different conditions for $\phi = 3$ % are shown. The figure suggests that the minimum Nu_{avg} of 10.87 corresponds to Re of 250 in the *PT* case and the maximum Nu_{avg} is 54.56 which corresponds to Re number of 1000 in the *RTT3* case; the difference between the minimum and maximum values of Nu_{avg} is 401.94 %. The values of Nu_{avg} for the aforementioned cases are also presented in Table 5. The table shows that similar to previous cases, the higher improvement made by increasing the Re number is dedicated to *PT* mode. For $\phi = 3$ %, the average improvement made by increasing the Re number from the minimum to its maximum is 56 %.

By comparing the percent enhancements made by increasing the Re number averaged between different working modes at each value of ϕ, it could be seen that the greatest improvement is for $\phi = 1$ %; the average percent improvement in cases of $\phi = 1$ %, 2 %, and 3 % are 76 %, 62 % and 56 %, respectively. In other words, although the Re increase would enhance the heat transfer in all cases of the heat exchanger and fluid types, the improvement is the highest in the case of $\phi = 1$ %. The average percent enhancements obtained by increasing the Re number from its minimum to maximum value are 76, 62, and 56 % for $\phi = 1$ %, 2 %, and 3 %, respectively. This shows that the Re number increase works best at the lowest ϕ. In fact, at higher values of ϕ, the effect of the Re number increase is not significantly effective on heat transfer enhancement. Similar to previous cases, using *NF* instead of pure water has the highest improving effect in the *PT* case and in other cases, the presence of tapes and their rotation works better.

- *The variation of average Nu numbe; the effect of NF concentration*

To reveal the heat transfer effect of varying ϕ, the Nu_{avg} is depicted versus ϕ in *PT* and *STT* working modes in Fig. 7(a) and (b), respectively. Fig. 7 (a) shows that for all Re numbers, the lowest Nu_{avg} corresponds to $\phi = 0$ % and the highest value is for $\phi = 3$ % which are of 10.08 and 19.10, respectively; this shows the maximum improvement of 89 % due to simultaneous use of *NF* and the Re number increase from their minimum to maximum values. The numerical values of Nu_{avg} for the studied Re numbers and ϕ values are listed in Table 6; also, the enhancement made by using $\phi = 3$ % instead of pure water is shown. By comparing Nu_{avg} versus ϕ for different *NF*s, the heat transfer improvement could be seen at all Re numbers with the highest improvement for Re = 500. By increasing ϕ from $\phi = 0$ to $\phi = 3$ %, Nu_{avg} is increased by 7.4 %, 9.9 %, 7.4 % and 7.1 % for Re = 250, 500, 750 and 1000, respectively.

Fig. 7 (b) shows Nu_{avg} versus ϕ for different Re numbers in the *STT case*. The figure shows that the lowest Nu_{avg} of 13.01 corresponds to $\phi =$ 0 % and Re = 250, and the maximum Nu_{avg} is 23.15, which corresponds to $\phi = 3$ % and Re = 1000. The difference between the maximum and minimum values of Nu_{avg} is 78 %. Table 6 shows the values of Nu_{avg} for

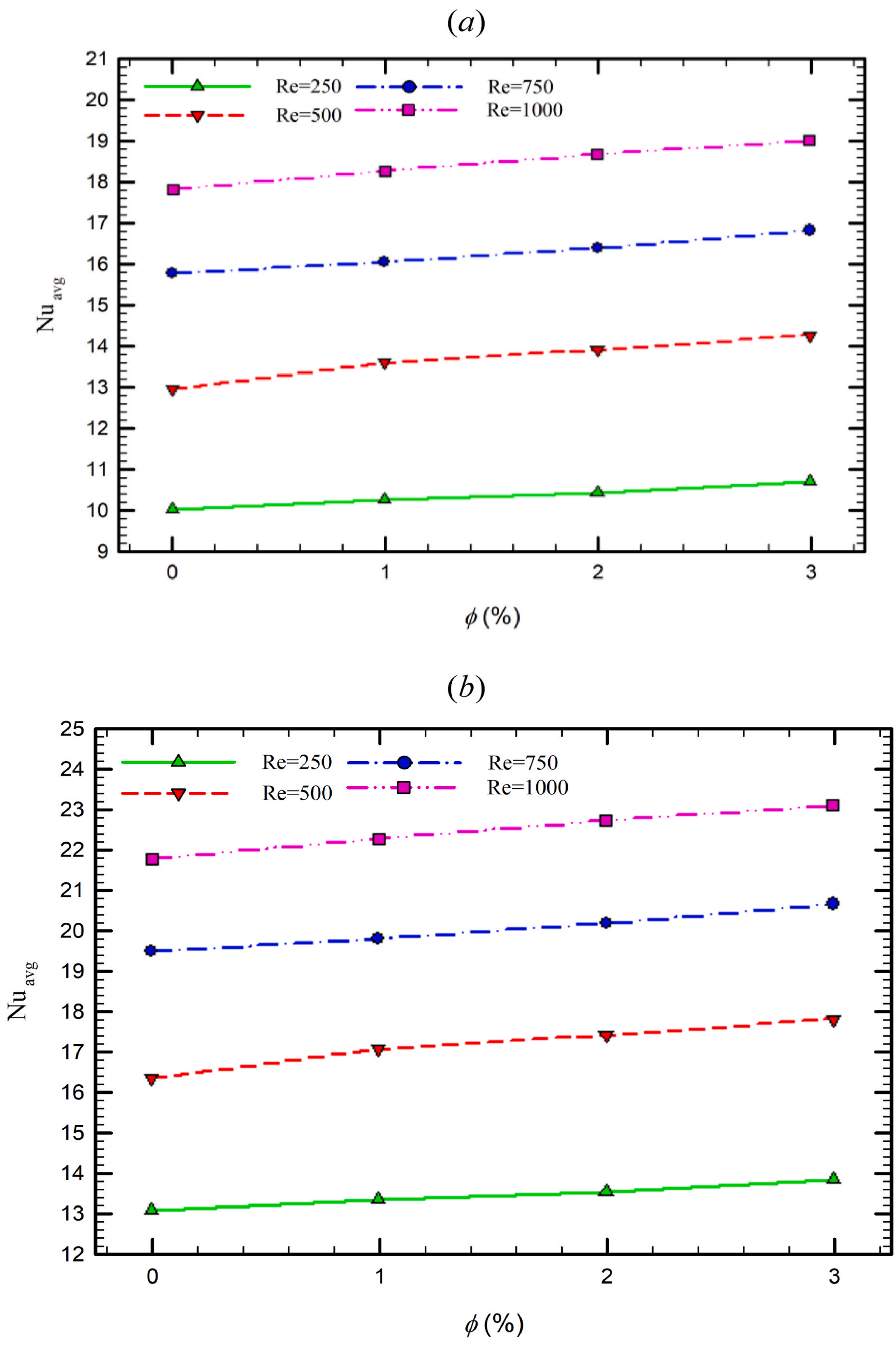

Fig. 7. Nu_{avg} versus ϕ in different Re numbers in a) *PT* and b) *STT cases*.

Table 6
Numerical values of Nu_{avg} in *PT* and *STT cases.*

ϕ (%)	PT case			
	R e			
	250	500	750	1000
0	10.079	13.052	15.807	17.820
1	10.248	13.498	15.9593	18. 299
2	10.538	13.981	16.4315	18.657
3	10.829	14.341	16.981	19.099
$\frac{\Delta Nu_{avg}}{Nu_{avg}}\%$	7.4	9.9	7.4	7.1
	STT case			
0	13.010	16.321	19.492	21.811
1	13.288	17.053	19.812	22.325
2	13.496	17.398	20.203	22.772
3	13.803	17.811	20.687	23.146
$\frac{\Delta Nu_{avg}}{Nu_{avg}}\%$	6.1	9.1	6.1	6.1

the investigated cases; also, the obtained enhancements resulting from using $\phi = 3$ % instead of pure water at different Re numbers are listed. As seen, by increasing ϕ, the average heat transfer coefficient increased at each Re number; by comparing the values of enhancements for the *PT* and *STT* cases, it could be seen that adding stationary twisted tapes attenuated the improving effect of *NF* on heat transfer. This could be attributed to the existence of induced secondary flow from the existence of the twisted tapes, which eventually downplays the improvement resulting from increasing ϕ [19]. However, similar to the *PT* case, the highest improvement as a result of increasing ϕ took place for Re number of 500.

Fig. 8 (a) shows Nu_{avg} versus the ϕ for *RTT1 case* at different Re numbers. In this case, (rotating tapes), similar to other cases (plain tube and stationary tapes), the overall trend of Nu_{avg} is increasing by the *NF* concentrations but, with a higher inclination rate. In the *STT* case and Re = 1000, by increasing ϕ from $\phi = 0$–4 %, Nu_{avg} increased by 6.1 %, while in the *RTT1 case*, it increased by 18.8 %. The improvement, which also exists for other Re numbers, verifies the great effect of tape rotation

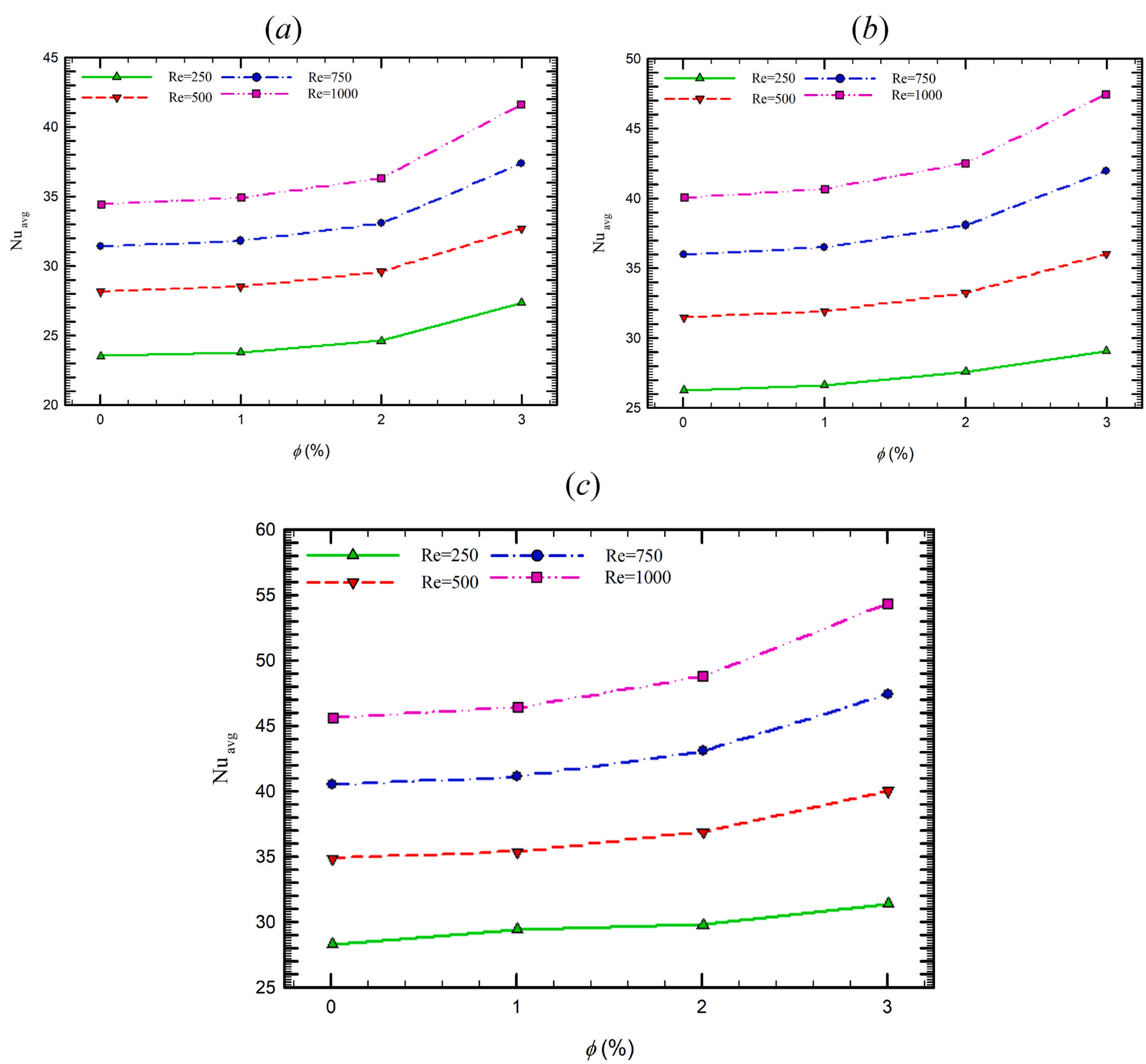

Fig. 8. $\boldsymbol{Nu_{avg}}$ versus $\boldsymbol{\phi}$ in different Re numbers in the *a) RTT1, b) RTT2* and *c) RTT3 cases.*

Table 7
Numerical values of Nu_{avg} in rotating modes; *RTT1, RTT2* and *RTT3 cases* for different Re numbers and $\boldsymbol{\phi}$

ϕ (%)	RTT			
	Re			
	250	500	750	1000
0	23.507	27.233	31.539	34.508
1	23.931	28.512	32.074	34.950
2	24.219	29.016	33.059	36.484
3	26.534	31.803	37.470	41.013
$\frac{\Delta Nu_{ave}}{Nu_{ave}}$ %	13.0	16.8	18.8	18.8
	RTT2			
0	26.242	31.462	36.000	40.122
1	26.581	31.911	36.544	40.750
2	27.575	33.232	38.142	42.620
3	29.056	36.046	42.029	47.573
$\frac{\Delta Nu_{ave}}{Nu_{ave}}$%	10.7	14.6	16.7	18.6
	RTT3			
0	28.470	34.809	40.499	45.689
1	29.301	35.527	41.120	46.491
2	29.869	36.900	43.111	48.877
3	31.466	40.022	47.505	54.557
$\frac{\Delta Nu_{ave}}{Nu_{ave}}$%	10.5	15.0	17.3	19.4

Table 8
Numerical values of $\boldsymbol{Nu_{avg}/Nu_{avg,PT}}$ in the *STT*, *RTT1*, *RTT2* and *RTT3 cases*.

ϕ (%)	STT case			
	Re			
	250	500	750	1000
0	1.29	1.25	1.233	1.223
1	1.296	1.263	1.241	1.22
2	1.28	1.244	1.229	1.22
3	1.274	1.241	1.218	1.211
	RTT1 case			
0	2.332	2.086	1.995	1.936
1	2.335	2.112	2.009	1.909
2	2.298	2.075	2.011	1.955
3	2.45	2.217	2.206	2.147
	RTT2 case			
0	2.603	2.41	2.277	2.251
1	2.593	2.364	2.289	2.226
2	2.616	2.376	2.321	2.284
3	2.683	2.513	2.475	2.49

on heat transfer improvement due to the ϕ increase. The figure shows that the lowest Nu_{avg} of 23.5 corresponds to pure water and Re = 2250 and the maximum one is 41.0, which is for $\phi = 3$ % and Re = 1000; this shows an improvement of 74 %. The values of Nu_{ave} for the investigated cases and the improvements as the result of increasing ϕ from $\phi = 0$–4 % for each Re number are listed in Table 7. It is seen that the enhancing effect of increasing ϕ at each Re number is increased as a result of tape rotation. This could be attributed to the more intensive collision of nano *HTF* that comes from the rotation of the tapes. Additionally, the Re number increment intenses the enhancing effect of the ϕ increase in this case, which was absent in the *STT* case, while the percent improvement as a result of increasing ϕ was almost fixed for all Re numbers in the *STT* case (except for Re = 500). The Re number increases from Re = 250 to 1000, and the percent improvement grows from 13 % to 18.8 %.

In Fig. 8 (b) the variations in Nu_{avg} versus ϕ for different Re numbers for the *RTT2 case,* are shown. As seen, by increasing the rotational speed of the tapes, Nu_{avg} increases at all ϕ values, but increasing ϕ is not as large as in the *RTT1 case*. In the *RTT1 case*, by increasing ϕ from $\phi = 0$ to $\phi = 4$ %, the Nu_{avg} increment is 13 % and 18.8 % for Re = 250 and 1000, which are 10.7 and 18.6 in *RTT2*, respectively. The minimum and maximum values of Nu_{avg} are 26.24 and 47.57, which correspond to ϕ and Re numbers of 0–4 % and 250–1000, respectively; additionally, the enhancement obtained by the simultaneous increase of ϕ and Re number from their minimum to maximum values is 81 %. In Table 8 the values of Nu_{avg} for the studied cases and the improvements as the result of the ϕ increase from $\phi =$ 0–4 % are shown. Similar to previous cases, increasing ϕ increases Nu_{ave} for each Re number, but despite the previous cases, the enhancement grows continuously by increasing the inlet Re number; by increasing the Re number from Re = 250 to 1000, $\frac{\Delta Nu_{ave}}{Nu_{ave}}$ % increased by 10.7–18.6. This verifies that at the tape rotational speed corresponding to the *RTT2 case*, the increase in the fluid flow rate intensifies the effect of ϕ increment with a higher inclination rate compared to the *RTT1 case*. This effect could be attributed to the intensifying effect of using *NF* at higher rotational speed and flow rates.

The variations in Nu_{avg} versus ϕ for different Re numbers in the *RTT3 case* are depicted in Fig. 8 (c). By comparing the Nu_{avg} in each case with the corresponding value in other cases (Table 9), the improving effect of rotation and the increased rotational speed on heat transfer coefficient could be seen; also, the improving effect of increasing the ϕ averaged between working conditions at different Re numbers has been diminished compared to *RTT1 case*. The average improvement of Nu_{avg} as the result of ϕ increment in the *RTT1 case* is 16.8 %, while the corresponding value in the *RTT3 case* is 15.5 %. This suggests that despite the heat transfer improvement by the ϕ increase, at conditions of high rotational speed, using the concentrated *NF* is not a determinant factor. In this case, the difference between the maximum and minimum values of Nu_{avg} is 92 %, which is highest among all other cases.

To reveal the improving effect of using the tapes and their rotation, the quotient of the *Nu* number at each Re number and ϕ to corresponding values in different cases are listed in Table 8. As could be seen in all cases, the value of $\frac{Nu_{avg}}{Nu_{avg,PT}}$ is higher than one and this show the improving effect of using the tapes on heat transfer rate. In addition, although using the tapes would improve the heat transfer coefficient, the improvement is not the same for different Re numbers and *NF* concentrations and decreased by increasing the values of Re numbers and ϕ; at *STT* case by increasing the Re number and *NF* concentration from 250 to 1000 and 0–4 %, the improvement depressed by 1.3 % and 5.2 %, respectively. Although, it saw a continuous decreasing trend of improvement versus the Re number increase versus increasing the ϕ an increasing-decreasing trend could be seen.

For *RTT1* case, it could be seen that the enhancement quotient increased and decreased by increasing the *NF* concentration and Re number, respectively. The value of $Nu_{avg}/Nu_{avg,PT}$ grows from 2.33 to 2.45 by increasing the ϕ value from 0 to 3 %; the increase of $Nu_{avg}/Nu_{avg,PT}$ versus the ϕ increment suggests that in *RTT case*, increasing ϕ has higher improving effect than in *PT case*. This fact which was also has been observed previously shows the more effective presence of *NP* in the *RTT1 case* which comes from the more intensive collision of *NPs* to heat transfer surfaces. On the other hand, the decreasing effect of Re number on $Nu_{avg}/Nu_{avg,PT}$ shows that the Re number increase is more effective in heat transfer improvement in *PT* rather than *RTT1 case*. This result which also was observed in the *STT case* suggests that using the internal tapes in stationary (*STT*) and rotating (*RTT1*) modes veils and turns down the Re number improving the effect on heat transfer coefficient enhancement; in other words, the Re number increase works best on heat transfer improvement in *PT* rather than the other cases.

The numerical values of $Nu_{avg}/Nu_{avg,PT}$ for different values of Re numbers and ϕ in Table 8 shows that by employing the rotated twisted tape in the *RTT2* case, the *Nu* number has grown up in all cases; as was expected, the highest and lowest quotients of $Nu_{avg}/Nu_{avg,PT}$ are

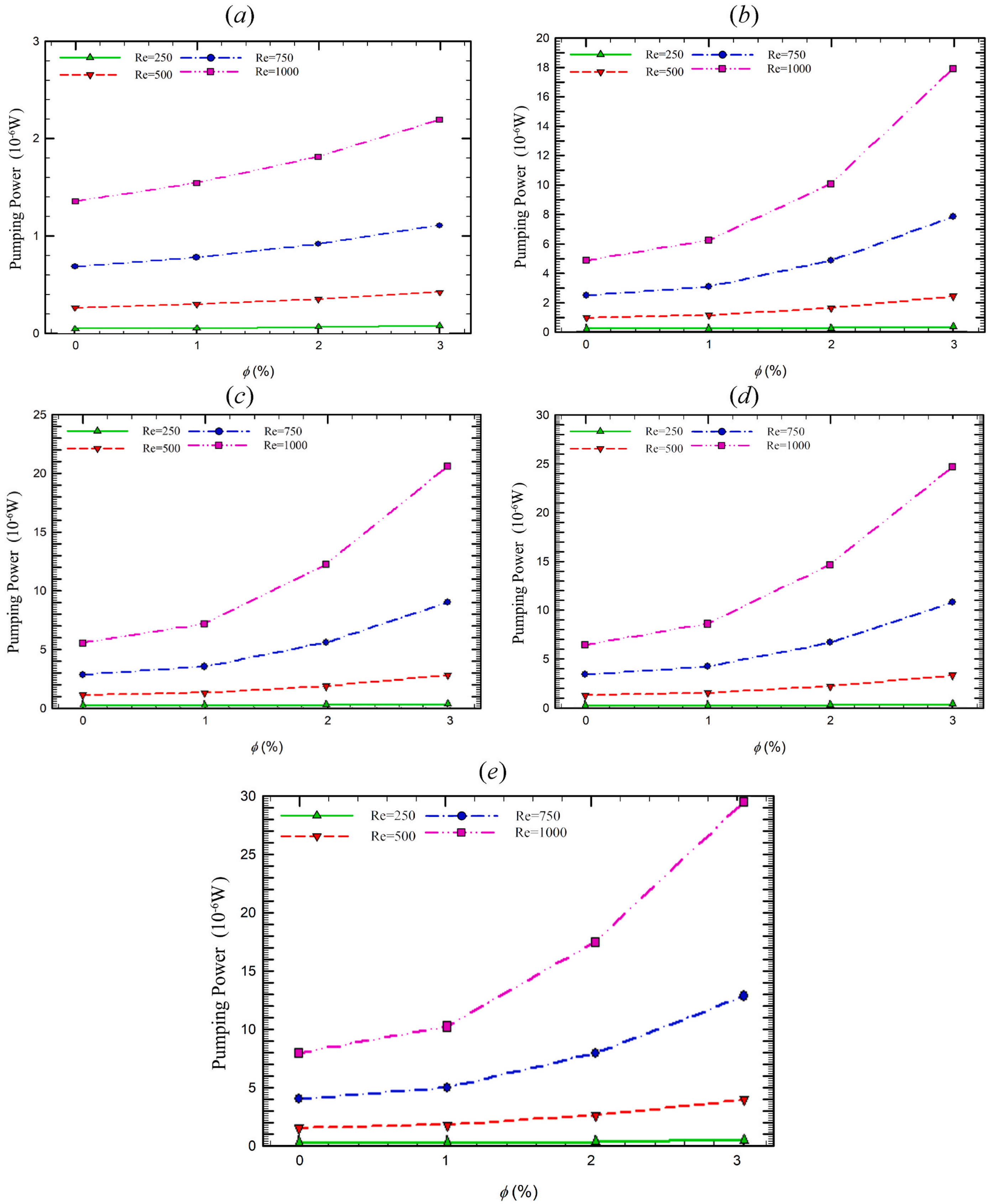

Fig. 9. $\dot{W}_{pump}$ versus ϕ for different Re numbers in *a) PT, b) STT, c) RTT1, d) RTT2* and *e) RTT3 cases.*

Table 9
Numerical values of $\dot{W}_{pump}$ (in μW) in *PT*, *STT*, *RTT1*, *RTT2*, and *RTT3 cases*.

ϕ (%)	*Re* 250	500	750	1000
PT case				
0	0.058	0.272	0.693	1.358
1	0.064	0.308	0.785	1.547
2	0.075	0.360	0.924	1.814
3	0.089	0.433	1.111	2.191
$\frac{\Delta \dot{W}}{W}\%$	53.4	59.2	60.3	61.3
STT case				
0	0.227	0.992	2.508	4.894
1	0.236	1.166	3.097	6.284
2	0.289	1.657	4.886	10.099
3	0.371	2.466	7.852	17.947
$\frac{\Delta \dot{W}}{W}\%$	63.4	148.6	213.0	266.7
RTT1 case				
0	0.245	1.136	2.869	5.578
1	0.271	1.336	3.547	7.195
2	0.331	1.896	5.593	12.238
3	0.428	2.822	8.991	20.547
$\frac{\Delta \dot{W}}{W}\%$	74.7	148.4	213.4	268.3
RTT2 case				
0	0.289	1.340	3.386	6.371
1	0.319	1.576	4.184	8.489
2	0.390	2.237	6.597	14.436
3	0.501	3.329	10.605	24.239
$\frac{\Delta \dot{W}}{W}$	73.3	148.4	213.2	280.4
RTT3 case				
0	0.348	1.614	4.079	7.964
1	0.385	1.898	5.040	10.228
2	0.470	1.695	7.949	17.393
3	0.604	4.012	12.777	29.203
$\frac{\Delta \dot{W}}{W}$	73.6	148.6	213.2	266.7

dedicated to pure water - Re = 250 and $\phi = 3\%$ - Re = 1000, respectively. The value of $Nu_{avg}/Nu_{avg,PT}$ in *RTT2 case* varies similar to that in the *RTT1 case* and the quotient increased by decreasing and increasing the values of Re and ϕ, respectively. Despite the similar variation versus the ϕ number, the ratio varies with a less intensity in *RTT2* rather than *RTT1 case*; at Re = 250, by increasing the ϕ from 0 to 3 %, the $Nu_{avg}/Nu_{avg,PT}$ increased by 3.2 % and 5.1 % in *RTT2* and *RTT1* cases, respectively. This result which is also repeated in other Re numbers, shows that at higher rotational speed the enhancing effect of increasing ϕ would be diminished.

By inspecting $Nu_{avg}/Nu_{avg,PT}$ in the *RTT3 case* for different values of ϕ and Re numbers, a similar trend to the previous case with a lower change rate could be observed; for pure water, by altering the Re number from 250 to 1000 the value of quotient decreased by 9.2 % which was 13.5 %, and 17 % for *RTT2* and *RTT1* cases, respectively. This result which is also repeated for the other ϕ s shows that by increasing the rotational speed of the tape, the effect of Re number increment on improving the heat transfer would be lessened [19].

4.2. The pumping power

Fig. 9(a)–(e) shows $\dot{W}_{pump}$ for different cases (*PT*, *STT*, *RTT1*, *RTT2*, and *RTT3 cases*) versus the ϕ, at different Re numbers. At *PT case*, minimum value of $\dot{W}_{pump}$, i.e. 0.058 μW corresponds to pure fluid (ϕ = 0) and Re = 250, and the maximum is 2.191 μW, which corresponds to ϕ = 3 % and Re = 1000. The numerical values of $\dot{W}_{pump}$ for the other investigated cases are listed in Table 9. The maximum $\dot{W}_{pump}$ in this case was observed to be 36.8 times the minimum value. It is also seen that at each Re number, by increasing ϕ, the required $\dot{W}_{pump}$ is increased. The increase of $\dot{W}_{pump}$ due to the ϕ increase could be attributed to increasing the fluid viscosity as the effect of *NP* presence is increased by the Re number increment. It can be seen in Fig. 9 that by increasing the Re number, the effect of ϕ increase on $\dot{W}_{pump}$ enlarged accordingly; by the ϕ increase from $\phi = 0$ to $\phi = 4$ % $\dot{W}_{pump}$ grows by 53.4 % and 61.3 % in case of Re = 250 and 1000, respectively. The slight increasing effect of the *NP* presence by the Re number increase could be attributed to more intensive contact of *NP*s, which increases the pressure loss at higher flow rates.

Fig. 9 (b) shows $\dot{W}_{pump}$ versus ϕ for different Re numbers for the *STT* case. The figure shows that the lowest and the highest $\dot{W}_{pump}$ corresponds to ϕ = 0 and Re = 250, and ϕ = 3% and Re = 1000, with the corresponding values of 0.227 and 17.947 μW, respectively; the values of $\dot{W}_{pump}$ for the other cases along with the power increment due to ϕ increase from ϕ = 0–4 % at each Re number, also shown in Table 9. The percent increment of $\dot{W}_{pump}$ due to the simultaneous Re number and ϕ increase is 7810 %, which is more than twice the corresponding value in the *PT* case (3680 %). This illustrates the deep effect of the employed twisted tapes on the factors that affect the $\dot{W}_{pump}$ (i.e., ϕ and Re number). This fact could also be seen by comparing the percentage of $\dot{W}_{pump}$ increment ($\frac{\Delta \dot{W}_{pump}}{\dot{W}_{pump}}\%$) due to ϕ increase from ϕ = 0–4 % for each Re number in cases of *PT* and *STT cases*. By comparing Fig. 9 (a) and 9 (b), it can be seen that in case of using stationary twisted tapes (*STT* case), increasing ϕ is more effective on $\dot{W}_{pump}$ than in the *PT* case. In the *PT* case and at Re = 1000, by increasing ϕ from 0 to 4 %, the $\dot{W}_{pump}$ increasing percent is 61.3 %, while the corresponding value in the *STT case* is 266.7 %. This behavior, which is seen at all Re numbers, is more pronounced at higher Re numbers. This could be explained by the secondary flow and increased flow path induced by the presence of twisted tapes; in this case, the increased viscosity resulting from the ϕ increment has the highest effect on the pressure loss and $\dot{W}_{pump}$.

Fig. 9 (c) shows $\dot{W}_{pump}$ in the *RTT1* case versus ϕ for different Re numbers; the corresponding numerical values are also listed in Table 9. By inspecting the variation of $\dot{W}_{pump}$, a similar trend is observed in the cases of *STT* and *RTT1*, and increasing ϕ increases $\dot{W}_{pump}$ in both cases. In addition, although the $\dot{W}_{pump}$ in the *RTT1 case* is higher than the corresponding values in the *STT* case, the $\dot{W}_{pump}$ enlargement due to the ϕ increment is nearly the same at each Re number. In the *RTT1* case, the lowest $\dot{W}_{pump}$ of 0.244 μW corresponds to ϕ = 0 % and Re = 250, and the maximum of 20.547 μW corresponds to ϕ = 3 % and Re = 1000. The difference between the maximum $\dot{W}_{pump}$ and minimum $\dot{W}_{pump}$ is 8287 %, which is slightly higher than the corresponding value in the *STT* case (7810 %). This shows that the tape rotation would intensify the increasing effect of ϕ and Re number, which is mainly due to the presence of the induced secondary flow. This time, the effect of tape rotation is more effective at the lowest Re number; in other words, except for a low Re number, the effect of ϕ increase on the $\dot{W}_{pump}$ increment is nearly equal for the *STT* and *RTT1* cases. This shows that at a high Re number, the induced secondary flows work equally in the *RTT1* and *STT cases* on increasing the $\dot{W}_{pump}$ due to ϕ increment.

Fig. 9 (d) shows the variation of $\dot{W}_{pump}$ versus ϕ in the *RTT2 case* for different Re numbers. It firstly shows the increasing effect of both Re number and *NF* concentration increase on pumping power; also, it shows the higher effect of *NF* concentration increase on $\dot{W}_{pump}$ at the highest Re number. $\dot{W}_{pump}$ varies between the minimum and maximum values of 0.289 and 24.24 μW*,* which shows a maximum change of 8287 %. By comparing the overall improvement made by the cumulative effect of increasing the ϕ and Re number with the previous case (*RTT1*), a sudden

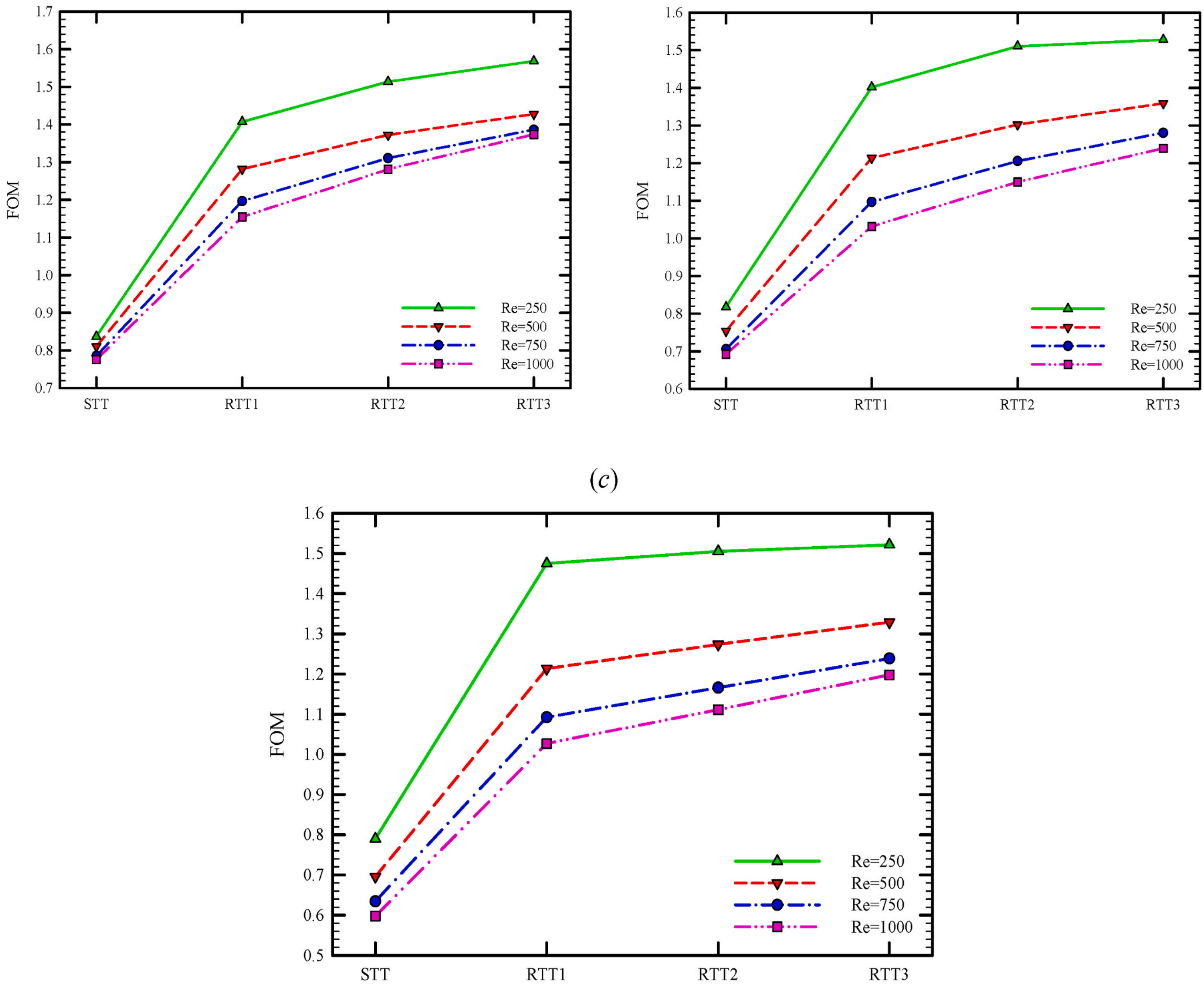

Fig. 10. The values of *FOM* for different cases for *a*) $\phi = 1$ %, *b*) 2 % and *c*) 3 %.

change could be observed; the maximum change in *STT* and *RTT1 cases* was 78 times, while here, the improvement is 83 times. This increasing effect of using *NF* instead of pure fluid grows at first by inserting the twisted tape (*STT* case versus the *PT* case) and secondly by increasing the rotational speed (from *RTT1* to *RTT2* cases). It seems that there is a specific speed around which the increasing effect of adding *NP*s on $\dot{W}_{pump}$ is the highest and before and after which, the resulting increment is less. Additionally, as seen in Table 10 and similar to the previous cases, the attenuating effect of using *NF* increases by increasing the Re number.

The variation of $\dot{W}_{pump}$ versus ϕ in the *RTT3* case for different Re numbers is depicted in Fig. 9 (e). According to this figure, the lowest and the highest $\dot{W}_{pump}$ are 0.348 and 29.203 μW, which correspond to $\phi =$ 0 % and Re = 250 and $\phi = 3$ % and Re = 100, respectively; therefore, the difference between the maximum and minimum $\dot{W}_{pump}$ in this mode is 8292 %. By comparing the maximum $\dot{W}_{pump}$ increments made by simultaneous increasing the ϕ and Re numbers in the *RTT2* and *RTT3* cases, it can be seen that the increments are nearly the same. In other words, using *NF* instead of the pure fluid and increasing ϕ has nearly the same effect on the growth of $\dot{W}_{pump}$. By inspecting $\dot{W}_{pump}$ in different cases, different ϕ and Re numbers in Tables 10 and it can be concluded that although increasing the Re number and ϕ would increase $\dot{W}_{pump}$ in each case but the effect of ϕ in $\dot{W}_{pump}$ is highest in *RTT case* and the lowest in *PT case*. Additionally, between three different rotating modes, the maximum $\dot{W}_{pump}$ increment due to *NF* concentration increase is dedicated to the *RTT2* case. In other words, between different cases, in the *RTT2* case, the effect of the ϕ increment on $\dot{W}_{pump}$ is the highest.

4.3. The overall performance of the system

Although the existence of twisted tapes in the fluid flow path improves heat transfer, it would also increases $\dot{W}_{pump}$. To determine which factor has the prominent effect (improving or destroying) on overall system performance, a unique parameter is used to consider both heat transfer and pressure drop increments simultaneously. The figure of merit (*FOM*) parameter, as defined in Eq. (21) is employed to evaluate the overall system performance. *FOM* values above 1 indicate increased thermal efficiency, and values below 1 show reduced system performance. Fig. 10(a)–(c) reveal the values of *FOM* in different geometric cases for different Re numbers and for $\phi = 1$ %, 2 %, and 3 %, respectively. As shown, for all the employed *NF*s, using rotated twisted tape, the value of *FOM* is always greater than one. In the case of stationary

Table 10
Numerical values of the *FOM* in the *STT*, *RTT1*, *RTT2* and *RTT3 cases*.

ϕ (%)	Re = 250	500	750	1000
	STT			
0	0.817	0.814	0.808	0.803
1	0.837	0.811	0.786	0.776
2	0.818	0.753	0.705	0.692
3	0.790	0.696	0.634	0.598
	RTT1			
0	1.416	1.309	1.243	1.214
1	1.408	1.282	1.197	1.155
2	1.402	1.214	1.097	1.032
3	1.522	1.214	1.093	1.027
	RTT2			
0	1.512	1.401	1.359	1.340
1	1.514	1.372	1.311	1.281
2	1.510	1.302	1.205	1.150
3	1.522	1.274	1.166	1.111
	RTT3			
0	1.535	1.457	1.437	1.420
1	1.569	1.428	1.386	1.374
2	1.569	1.359	1.280	1.239
3	1.522	1.329	1.239	1.198

twisted tapes (*STT* case), the value of *FOM* is always under 0.9, which eliminates the proper application of the stationary twisted tapes. In other words, despite the heat transfer enhancing effect of using the stationary twisted tapes, the increased pressure loss eliminates it. Also, the *FOM* lessens by increasing the *NF* concentration which is due to a higher viscosity increase than that of the heat transfer coefficient. This shows the necessity of employing other heat transfer-improving factors such as the rotation of tapes.

In rotating twisted tape modes (*RTT1*, *RTT2*, and *RTT3* cases), the *FOM* is greater than one but, by increasing ϕ *FOM* alleviated accordingly. The numerical values of *FOM* for the *STT*, *RTT1*, *RTT2*, and *RTT3* cases are listed in Table 10. By inspecting, it can be seen that *FOM* decrement due to the ϕ increase is more prominent at higher Re numbers, and at low Re numbers, it does not change considerably. For example, in the *RTT3 case,* by increasing ϕ from 0 to 4 %, the *FOM* alleviated by only 0.8 % at Re = 250, while the decrement was 15.6 % for Re = 1000. This indicates the higher improving effect of *NP* presence on heat transfer improvement rather than its deteriorating effect on pressure loss at lower Re numbers, which works reversely at high Re numbers. In other words, under the conditions of the present study, it would be more beneficial to use the lowest ϕ (1 %) at the highest rotational speed state (*RTT3* case).

The effect of increasing the Re number on the pressure loss and $\dot{W}_{pump}$ is more prominent than its effect on heat transfer improvement. The deteriorating effect of increasing the Re number on the *FOM* becomes greater at higher ϕ and is very small for the pure fluid ($\phi =$ 0 %). For example, in the *RTT3 case*, increasing the Re number from 250 to 1000 decreases the *FOM* by 7.1 % and 21 % in cases of $\phi =$ 0 % and 3 %, respectively. This indicates that the best working condition could be achieved at the lowest ϕ ($\phi =$ 1 %), which also gives flexibility for employing a wider range of flow rates (Re numbers) without losing the value of *FOM* significantly (See Table 10).

5. Conclusion

This study analyzes the flow characteristics of an elliptical duct heat exchanger equipped with twisted tapes in two different modes of stationary and rotating states and three rotational speeds using *NF* as the *HTF*. The obtained results show the improving effect of incorporating *NP* on heat transfer rate which increases by the *NP* concentration increment and is prominent in rotating rather than *STT* and *PT cases.* Additionally, the Nu_{avg} change due to increasing ϕ is lower at low Re numbers and becomes higher at high Re numbers. The effect of the Re number increase on altering Nu_{avg} is not the same in different cases; in the *PT case*, increasing the Re number has the largest effect on the value of Nu_{avg} while, it is the smallest in the *RTT case.* This shows the necessary and significant effect of NP presence in cases where the other improving effect are absent. The Re number increase works best on heat transfer improvement at the lowest ϕ values. Increasing ϕ, also increases $\dot{W}_{pump}$ and the increment percentage of $\dot{W}_{pump}$ due to the simultaneous effect of Re number and ϕ increase in the *STT case* is higher than twice the corresponding value in the *PT case.* Between the study cases, the increasing effect of ϕ in $\dot{W}_{pump}$ is the most in rotating (*RTT*) modes and the least in the *PT case.* Additionally, between three different rotating modes, the maximum $\dot{W}_{pump}$ increment due to ϕ increase is for the *RTT2 case.* In cases of rotated twisted tape mode, *FOM* is always greater than one. In the *STT case*, the value of *FOM* is always below 0.9, which eliminates the good application of stationary twisted tapes. Increasing the Re number reduces the *FOM* while increasing ϕ improves it. This fact approves again the significant application of *NF* in overall system performance improvement. In the *RTT3 case*, increasing the Re number from 250 to 1000 decreases the *FOM* by 7.1 % and 21 % in cases of $\phi = 0$ % and 3 %, respectively. The highest value of *FOM* is 1.57, which is for the highest rotational speeds, the lowest Re number, and $\phi = 1$ %.

CRediT authorship contribution statement

Hassan Wathiq Ayoob: Data curation, Formal analysis. **Ihab Omar:** Supervision, Writing – review & editing. **Wed khalid Ghanim:** Methodology, Project administration. **Soheil Salahshour:** Supervision, Writing – review & editing. **Mohammad N. Fares:** Conceptualization, Data curation, Formal analysis. **Mohammad Ali Fazilati:** Formal analysis, Writing – original draft, Conceptualization, Data curation, Formal analysis. **Sh. Esmaeili:** Conceptualization, Data curation, Formal analysis.

Declaration of competing interest

The authors declare that they have no known competing financial interests or personal relationships that could have appeared to influence the work reported in this paper.

Data availability

No data was used for the research described in the article.

References

[1] S.-R. Yan, M.A. Fazilati, R. Boushehri, E. Mehryaar, D. Toghraie, Q. Nguyen, et al., Experimental analysis of a new generation of membrane liquid desiccant air-conditioning (LDAC) system with free convection of desiccant for energy economic management, J. Energy Storage 29 (2020) 101448.
[2] Y. Ma, M.A. Fazilati, A. Sedaghat, D. Toghraie, P. Talebizadehsardari, Natural convection energy recovery loop analysis, part I: energy and exergy studies by varying inlet air flow rate, Heat Mass Tran. 56 (5) (2020) 1685–1695.
[3] K.S. Dehkordi, M.A. Fazilati, A. Hajatzadeh, Surface Scraped Heat Exchanger for cooling Newtonian fluids and enhancing its heat transfer characteristics, a review and a numerical approach, Appl. Therm. Eng. 87 (2015) 56–65.
[4] S. Rainieri, F. Bozzoli, L. Cattani, P. Vocale, Parameter estimation applied to the heat transfer characterisation of Scraped Surface Heat Exchangers for food applications, J. Food Eng. 125 (2014) 147–156.
[5] W. Tu, Y. Tang, J. Hu, Q. Wang, L. Lu, Heat transfer and friction characteristics of laminar flow through a circular tube with small pipe inserts, Int. J. Therm. Sci. 96 (2015) 94–101.
[6] W. Tu, Y. Tang, B. Zhou, L. Lu, Experimental studies on heat transfer and friction factor characteristics of turbulent flow through a circular tube with small pipe inserts, Int. Commun. Heat Mass Tran. 56 (2014) 1–7.
[7] R. Manglik, A. Bergles, Heat Transfer and Pressure Drop Correlations for Twisted-Tape Inserts in Isothermal Tubes: Part I—Laminar Flows, 1993.

[8] R.M. Manglik, A.E. Bergles, Heat Transfer and Pressure Drop Correlations for Twisted-Tape Inserts in Isothermal Tubes: Part II—Transition and Turbulent Flows, 1993.

[9] P. Li, P. Liu, Z. Liu, W. Liu, Experimental and numerical study on the heat transfer and flow performance for the circular tube fitted with drainage inserts, Int. J. Heat Mass Tran. 107 (2017) 686–696.

[10] A. Fan, J. Deng, J. Guo, W. Liu, A numerical study on thermo-hydraulic characteristics of turbulent flow in a circular tube fitted with conical strip inserts, Appl. Therm. Eng. 31 (14–15) (2011) 2819–2828.

[11] N Sina, Aa Alizadeh, F Soltani, MA Fazilati, Prediction the dynamic viscosity of a new non-Newtonian hybrid nanofluid using experimental and Artificial Neural Network (ANN), methods 51 (15) (2020) 1351–1362.

[12] A. Dewan, P. Mahanta, K.S. Raju, P.S. Kumar, Review of passive heat transfer augmentation techniques, Proc. Inst. Mech. Eng. A J. Power Energy 218 (7) (2004) 509–527.

[13] P. Murugesan, K. Mayilsamy, S. Suresh, P. Srinivasan, Heat transfer and pressure drop characteristics in a circular tube fitted with and without V-cut twisted tape insert, Int. Commun. Heat Mass Tran. 38 (3) (2011) 329–334.

[14] P. Murugesan, K. Mayilsamy, S. Suresh, Turbulent heat transfer and pressure drop in tube fitted with square-cut twisted tape, Chin. J. Chem. Eng. 18 (4) (2010) 609–617.

[15] S. Eiamsa-Ard, P. Promvonge, Performance assessment in a heat exchanger tube with alternate clockwise and counter-clockwise twisted-tape inserts, Int. J. Heat Mass Tran. 53 (7–8) (2010) 1364–1372.

[16] S. Eiamsa-ard, K. Wongcharee, P. Eiamsa-Ard, C. Thianpong, Heat transfer enhancement in a tube using delta-winglet twisted tape inserts, Appl. Therm. Eng. 30 (4) (2010) 310–318.

[17] M. Bhuiya, M. Chowdhury, M. Saha, M. Islam, Heat transfer and friction factor characteristics in turbulent flow through a tube fitted with perforated twisted tape inserts, Int. Commun. Heat Mass Tran. 46 (2013) 49–57.

[18] J. Guo, A. Fan, X. Zhang, W. Liu, A numerical study on heat transfer and friction factor characteristics of laminar flow in a circular tube fitted with center-cleared twisted tape, Int. J. Therm. Sci. 50 (7) (2011) 1263–1270.

[19] Y.-Q. Song, N. Izadpanahi, M.A. Fazilati, Y.-P. Lv, D. Toghraie, Numerical analysis of flow and heat transfer in an elliptical duct fitted with two rotating twisted tapes, Int. Commun. Heat Mass Tran. 125 (2021) 105328.

[20] M. Rahimi, S.R. Shabanian, A.A. Alsairafi, Experimental and CFD studies on heat transfer and friction factor characteristics of a tube equipped with modified twisted tape inserts, Chem. Eng. Process: Process Intensif. 48 (3) (2009) 762–770.

[21] M. Jafaryar, M. Sheikholeslami, Z. Li, CuO-water nanofluid flow and heat transfer in a heat exchanger tube with twisted tape turbulator, Powder Technol. 336 (2018) 131–143.

[22] M.H. Esfe, H. Mazaheri, S.S. Mirzaei, E. Kashi, M. Kazemi, M. Afrand, Effects of twisted tapes on thermal performance of tri-lobed tube: an applicable numerical study, Appl. Therm. Eng. 144 (2018) 512–521.

[23] C. Qi, G. Wang, Y. Yan, S. Mei, T. Luo, Effect of rotating twisted tape on thermo-hydraulic performances of nanofluids in heat-exchanger systems, Energy Convers. Manag. 166 (2018) 744–757.

[24] Y. He, L. Liu, P. Li, L. Ma, Experimental study on heat transfer enhancement characteristics of tube with cross hollow twisted tape inserts, Appl. Therm. Eng. 131 (2018) 743–749.

[25] M. Bahiraei, N. Mazaheri, F. Aliee, M.R. Safaei, Thermo-hydraulic performance of a biological nanofluid containing graphene nanoplatelets within a tube enhanced with rotating twisted tape, Powder Technol. 355 (2019) 278–288.

[26] M.A.E.-M. Mohamed, A. Meana-Fernández, J.M. González-Caballín, A. Bowman, A. J. Gutiérrez-Trashorras, Numerical study of a heat exchanger with a rotating tube using nanofluids under transitional flow, Processes 12 (1) (2024) 222.

[27] V. Ghazanfari, A. Taheri, Y. Amini, F. Mansourzade, Enhancing heat transfer in a heat exchanger: CFD study of twisted tube and nanofluid (Al2O3, Cu, CuO, and TiO2) effects, Case Stud. Therm. Eng. 53 (2024) 103864.

[28] Y. Rao, Z. Shao, A. Rahimi, A. Kasaeipoor, E. Hasani Malekshah, Study on fluid flow and heat transfer in fluid channel filled with KKL model-based nanofluid during natural convection using FVM, Int. J. Numer. Methods Heat Fluid Flow 29 (8) (2019) 2622–2641.

[29] T.L. Bergman, A.S. Lavine, F.P. Incropera, D.P. DeWitt, Introduction to Heat Transfer, John Wiley & Sons, 2011.

[30] S. Rashidi, M. Akbarzadeh, N. Karimi, R. Masoodi, Combined effects of nanofluid and transverse twisted-baffles on the flow structures, heat transfer and irreversibilities inside a square duct–a numerical study, Appl. Therm. Eng. 130 (2018) 135–148.

[31] P. Barnoon, D. Toghraie, B. Mehmandoust, M.A. Fazilati, S.A. Eftekhari, Comprehensive study on hydrogen production via propane steam reforming inside a reactor, Energy Rep. 7 (2021) 929–941.